Reliability Analysis of Rolling Bearings Using a Weighted Nonlinear Mixed-Effects Degradation Model

Hung-Tse Hsu[1] Cheng-Jyun Shih[1]

[1] *Department of Statistics, National Cheng Kung University, Tainan 701, Taiwan*
jason28913788@gmail.com, moshen2250@gmail.com

ABSTRACT

Reliability assessment of rolling element bearings is critical for the predictive maintenance of industrial rotary machinery. This study proposes a Quadratic-Exponential Weighted Model (QEWM) based on Nonlinear Mixed-Effects (NLME) to characterize the degradation process of bearings. Utilizing the IMS Bearing Dataset (Set No. 2), we define the failure threshold based on the latest ISO 20816-3:2022 vibration severity standards, setting the critical RMS limit at 0.4 mm/s for Zone D. Unlike traditional models, the proposed QEWM incorporates a weight function to address heteroscedasticity, which typically intensifies during the rapid degradation phase. Model comparison based on the Akaike Information Criterion (AIC) demonstrates that QEWM significantly outperforms linear and unweighted quadratic models. To quantify the uncertainty of the estimation, a parametric bootstrap method with 5,000 replications was employed. The results identify a B10 life ($t_{0.1}$) of 165.3 hours, supported by a precise 95% confidence interval of $[162.7, 168.6]$ hours. This research provides a robust statistical framework for bearing life prediction that aligns with international industrial standards, ensuring high precision in prognostic assessments.

1. INTRODUCTION

Rolling element bearings are critical components in industrial rotary machinery, and their degradation behavior plays a decisive role in system reliability and maintenance planning. Unexpected bearing failures may lead to severe economic losses, safety risks, and unplanned downtime. Consequently, bearing prognostics and reliability assessment have been long-standing research topics in the field of Prognostics and Health Management (PHM).

In recent years, degradation-based approaches have become a mainstream methodology (Meeker, Escobar, & Pascual, 2021) for bearing life prediction. Instead of relying solely on failure time data, degradation models utilize condition monitoring signals, such as vibration measurements, to characterize the gradual deterioration process and estimate the remaining useful life. These approaches are particularly attractive for practical PHM applications, as they enable early fault detection and continuous reliability updating.

However, bearing degradation processes often exhibit complex characteristics that challenge conventional modeling assumptions (Meng, Li, Yin, & Pan, 2020). Empirical studies have shown that degradation trajectories typically display a clear phase transition: an early stage with relatively stable or slowly varying behavior, followed by a late stage with rapidly accelerating deterioration prior to failure. A single-stage degradation model is often insufficient to capture both regimes simultaneously, leading to biased parameter estimation and unreliable life prediction.

In addition to phase transition, bearing degradation data frequently exhibit pronounced heteroscedasticity. As vibration severity increases during the late degradation stage, the variability of observed signals also expands substantially. Many existing degradation models implicitly assume homoscedastic errors (Meeker et al., 2021), which may cause the estimation procedure to be dominated by high-variance observations in the late stage, thereby distorting the inferred degradation dynamics and uncertainty quantification.

To address these challenges, this study proposes a two-stage nonlinear mixed-effects degradation model with a variance-weighted structure. The first stage captures the gradual baseline degradation under relatively stable operating conditions, while the second stage introduces an exponential acceleration component activated after a change point. To accommodate the observed heteroscedasticity, a weighted variance function is incorporated into the model, allowing the residual variability to scale with the predicted degradation level. Furthermore, random effects are introduced to explicitly account for bearing-to-bearing variability.

The proposed modeling framework is applied to the IMS rolling bearing dataset, with failure defined according to the

ISO 20816-3:2022 vibration severity standard (International Organization for Standardization, 2022). Model performance is evaluated through information-criterion-based comparison and residual diagnostics. To quantify lifetime uncertainty, Monte Carlo simulation and bootstrap techniques are employed to derive reliability distributions and confidence intervals (Efron & Tibshirani, 1994; Rubinstein & Kroese, 2017). The results demonstrate that the proposed approach provides a robust and interpretable framework for bearing reliability assessment, aligning well with practical PHM requirements and industrial standards (Lee et al., 2014).

2. DATASET AND FAILURE DEFINITION

2.1. IMS Bearing Dataset

The proposed methodology is evaluated using the well-known IMS rolling bearing dataset (IMS Center, 2004), provided by the NSF Industry Cooperative Research Center for Intelligent Maintenance Systems (IMS) in collaboration with Rexnord Corporation. The experimental setup consists of four rolling bearings operating under constant conditions, including a rotational speed of 2000 RPM and a radial load of 6000 lbs, with forced lubrication applied throughout the experiment.

In this study, Dataset No. 2 is selected for analysis. The dataset spans from February 12 to February 19, 2004, and contains 984 data files recorded at 10-minute intervals. Each file includes one-second vibration signals sampled at 20 kHz from four bearings. During the observation period, Bearing 1 experienced failure, while Bearings 2–4 did not fail and are therefore treated as right-censored units. Furthermore, as the final two observations were recorded during machine shutdown, their vibration magnitudes do not reflect actual operational degradation characteristics. To avoid bias in subsequent modeling and lifetime inference, these anomalies were excluded from the analysis. Overall, this dataset provides a representative scenario for degradation-based reliability analysis involving both failed and censored components.

2.2. Feature Extraction

To characterize the degradation process, the root mean square (RMS) of the vibration signal is adopted as the degradation indicator. For each bearing and each observation time, the RMS is computed as

$$\mathrm{RMS} = \sqrt{\frac{1}{N}\sum_{j=1}^{N} x_j^2} \tag{1}$$

where x_j denotes the vibration signal amplitude at the j-th sampling point and $N = 20480$ is the number of samples within each signal segment.

RMS is widely used in bearing condition monitoring due to its strong association with vibration energy and mechanical wear (Wang & Gao, 2006). As bearing defects develop and propagate, vibration amplitudes increase, leading to a systematic rise in RMS values. These properties make RMS a suitable and interpretable degradation feature for reliability modeling.

2.3. Failure Definition

Bearing failure is defined using a threshold-based first-passage-time criterion (Meeker et al., 2021). Specifically, the failure time T is defined as the earliest time at which the RMS degradation indicator, $\mathrm{RMS}(t)$, exceeds a predefined critical threshold ω:

$$T = \inf\{t \mid \mathrm{RMS}(t) \geq \omega\} \tag{2}$$

The failure threshold is determined according to the ISO 20816-3:2022 vibration severity standard (International Organization for Standardization, 2022). Under this standard, vibration levels entering Zone D are generally regarded as dangerous and indicative of unacceptable operating conditions. Empirical guidelines suggest that Zone D vibration levels are approximately 4.5 to 5 times higher than the baseline vibration level corresponding to Zone A.

Based on the observed initial RMS values of the bearings, which average approximately 0.08 mm/s, the failure threshold is set to 0.4 mm/s in this study. Accordingly, the lifetime of each bearing is defined as the first passage time at which the RMS trajectory crosses this threshold. Bearings that do not reach the threshold within the observation window are treated as right-censored in the subsequent analysis.

Figure 1 shows the RMS degradation paths of four bearings over time. Each line represents the degradation trajectory of one bearing, with the time on the x-axis and the RMS value (in mm/s) on the y-axis. The failure time for Bearing 1 is indicated, defined as the time at which the RMS exceeds the threshold of 0.4 mm/s, marking the point of failure.

The remaining bearings (Bearing 2 to Bearing 4) have not reached the failure threshold within the observed time window, and are therefore treated as right-censored units. These paths highlight the gradual increase in vibration severity as degradation progresses, with Bearing 1 exhibiting a clear upward trend leading to failure. In contrast, the other bearings show varying levels of degradation without reaching the failure threshold, illustrating the heterogeneity in the degradation behaviors of the bearings.

3. TWO-STAGE NONLINEAR MIXED-EFFECTS DEGRADATION MODEL

3.1. Motivation for Two-Stage Modeling

Exploratory analysis of the RMS degradation paths reveals a clear phase-dependent behavior. During the early stage of operation, the vibration levels remain relatively stable or increase slowly, reflecting gradual wear under normal operat-

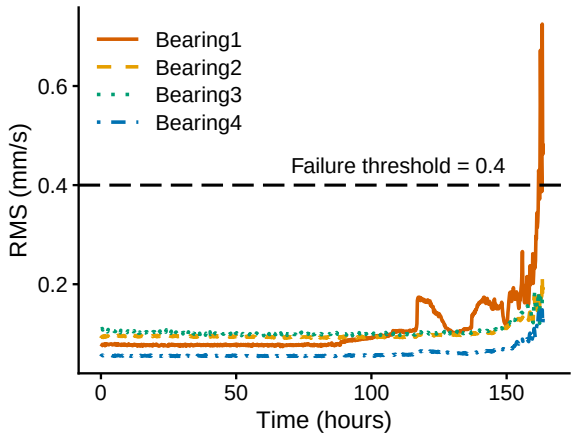

Figure 1. RMS degradation paths of the four bearings.

ing conditions. As the bearing approaches failure, however, the degradation process transitions into a rapidly accelerating stage characterized by a sharp increase in vibration severity.

Such phase-transition behavior is difficult to capture using a single-stage degradation model. Models that are sufficiently flexible to describe the late-stage acceleration often overfit the early-stage data, while simpler models that perform well in the early stage fail to represent the rapid deterioration near failure. These observations motivate the adoption of a two-stage degradation framework (Lin, Liao, Chen, & Yin, 2021), in which different mechanisms dominate the degradation process before and after a change point.

In addition, bearings operating under identical conditions may exhibit substantial variability in both initial vibration levels and degradation rates due to manufacturing tolerances, material imperfections, and installation differences. To explicitly account for this bearing-to-bearing heterogeneity, a mixed-effects modeling framework is employed (Lindstrom & Bates, 1990).

3.2. Model Formulation

Let $Y_i(t)$ denote the RMS degradation measurement of i bearing at time t. The proposed two-stage degradation model is defined as

$$Y_i(t) = \begin{cases} D_{1,i}(t) + \varepsilon_i(t), & t \le \tau, \\ D_{1,i}(\tau) + D_{2,i}(t) + \varepsilon_i(t), & t > \tau, \end{cases} \tag{3}$$

where τ represents the change point separating the early and late degradation stages, $D_{1,i}(t)$ denotes the baseline degradation trajectory in the early stage, $D_{2,i}(t)$ represents the additional degradation component activated after the change point, and $\varepsilon_i(t)$ is the random error term.

This formulation ensures continuity of the degradation path at $t = \tau$, thereby avoiding unrealistic discontinuities at the transition between stages.

3.3. Early-Stage Degradation Model

The early-stage degradation is modeled using a quadratic polynomial function:

$$D_{1,i}(t) = \alpha_{0,i} + \alpha_{1,i}t + \alpha_{2,i}t^2 \tag{4}$$

This formulation allows the model to capture mild curvature in the early degradation phase while maintaining sufficient flexibility to describe gradual changes in vibration severity. The adoption of a change-point framework ensures that the early-stage polynomial structure remains focused on characterizing baseline degradation, effectively decoupling it from the subsequent rapid acceleration phase. This prevents the relatively stable early-stage data from being influenced by the high-magnitude observations near failure, which often lead to biased parameter estimation in single-stage models.

3.4. Late-Stage Acceleration Model

To describe the rapid deterioration observed near failure, the late-stage degradation component is modeled using an exponential function:

$$D_{2,i}(t) = \theta \left(e^{\alpha_{3,i}(t-\tau)} - 1 \right). \tag{5}$$

This component represents an acceleration mechanism that is activated only after the change point. The exponential term depends on the elapsed time since the transition, $t - \tau$, ensuring that the acceleration effect is absent during the early stage. The subtraction of 1 guarantees that $D_{2,i}(\tau) = 0$, thereby preserving continuity of the degradation trajectory at the change point.

The exponential structure reflects the rapid escalation of vibration severity commonly associated with defect propagation and surface damage in rolling bearings as failure approaches (Gebraeel, Lawley, Li, & Ryan, 2005).

3.5. Random Effects Structure

To capture bearing-specific variability, model parameters are decomposed into fixed and random effects:

$$\alpha_{k,i} = \beta_k + b_{k,i}, \quad k = 0, 1, 2, 3, \tag{6}$$

where β_k denotes the population-level fixed effect for the k-th parameter and $b_{k,i}$ represents the bearing-specific random effect. The random effects vector

$$\mathbf{b}_i = (b_{0,i},\, b_{1,i},\, b_{2,i},\, b_{3,i})^\top$$

is assumed to follow a multivariate normal distribution with mean zero and covariance matrix $\mathbf{\Sigma}$.

This formulation allows different bearings to exhibit distinct

initial vibration levels, early-stage degradation trends, and late-stage acceleration rates, while still sharing a common population-level degradation structure.

4. VARIANCE WEIGHTING AND PARAMETER ESTIMATION

4.1. Evidence of Heteroscedasticity

Preliminary residual diagnostics based on unweighted two-stage models reveal a clear violation of the homoscedasticity assumption. Specifically, the magnitude of residuals increases systematically with the predicted RMS level, forming a pronounced funnel-shaped pattern. This phenomenon becomes particularly evident during the late degradation stage, where vibration severity escalates rapidly.

Such heteroscedastic behavior is commonly observed in vibration-based degradation data (Davidian & Giltinan, 1995). As bearing defects propagate and mechanical damage accumulates, vibration signals not only increase in magnitude but also become inherently more unstable. Consequently, treating the residual variance as constant across time may lead to inefficient parameter estimation and distorted uncertainty quantification, as late-stage observations with inflated variance exert disproportionate influence on the fitting process.

These observations motivate the incorporation of a variance structure that explicitly accounts for heteroscedasticity within the degradation modeling framework.

4.2. Weighted Variance Structure

To address the observed heteroscedasticity, a variance-weighted formulation is adopted (Davidian & Giltinan, 1995). The error term $\varepsilon_i(t)$ is assumed to follow a normal distribution with mean zero and variance that depends on the predicted degradation level:

$$\varepsilon_i(t) \sim \mathcal{N}\left(0, \sigma^2 |\hat{Y}_i(t)|^{2\delta}\right), \tag{7}$$

where $\hat{Y}_i(t)$ denotes the model-predicted RMS value at time t, σ^2 is a scale parameter, and δ is a power parameter governing the strength of variance inflation.

Under this formulation, observations associated with higher predicted vibration levels are allowed to exhibit larger variability. During parameter estimation, these high-variance observations are automatically assigned lower weights through the weighted likelihood, preventing them from dominating the estimation procedure. Importantly, this weighting mechanism is not an ad hoc adjustment but an integral component of the statistical model.

It should be emphasized that this approach does not eliminate heteroscedasticity in the original data. Instead, it explicitly models the variance structure so that the standardized residuals exhibit approximately constant variance, thereby restoring the validity of likelihood-based inference.

4.3. Change-Point Selection

The change point τ plays a critical role in defining the transition between early-stage and late-stage degradation. Directly estimating τ jointly with other model parameters often leads to numerical instability due to strong parameter dependence. To ensure robust estimation, τ is treated as a tuning parameter and selected via grid search.

Specifically, a candidate range for τ is specified based on exploratory analysis of degradation trajectories. For each candidate value, the two-stage nonlinear mixed-effects model is fitted while holding τ fixed. To maintain consistency with the subsequent model selection process, the Akaike Information Criterion (AIC) is employed as the objective function for the grid search (Akaike, 1974). While AIC and log-likelihood are equivalent for selecting τ when the number of parameters remains constant, utilizing AIC provides a unified framework for both change-point optimization and the comparison of different mean and variance structures (Akaike, 1974; Davidian & Giltinan, 1995). The value of τ that minimizes the AIC is selected as the optimal change point.

This procedure prioritizes structural model adequacy over precise inference on τ, aligning with the primary objective of reliable degradation and lifetime modeling.

4.4. Parameter Estimation Procedure

Model parameters are estimated using maximum likelihood estimation (MLE) within a nonlinear mixed-effects framework. Conditional on the optimal change-point τ selected via the grid search, the population fixed effects, the covariance matrix of the random effects, and the variance parameters of the error term are estimated jointly. The weighted variance structure is incorporated directly into the likelihood function, allowing both the mean and variance components to be optimized simultaneously. The overall estimation follows a standard nonlinear mixed-effects modeling approach (Lindstrom & Bates, 1990), where heteroscedasticity is accommodated through a variance function, and the marginal likelihood is approximated via linearization. To quantify parameter uncertainty and its subsequent impact on lifetime prediction, bootstrap techniques are employed.

For practical engineering applications and algorithmic implementation, the estimation procedure for the proposed QEWM is performed utilizing the `nlme` package in R. To ensure mathematical continuity of the two-stage degradation trajectory across the change-point τ, the operational time vector t is transformed into an early-stage baseline duration $t_h = \min(t, \tau)$ and a post-transition acceleration duration $t_f = \max(0, t - \tau)$ prior to model fitting.

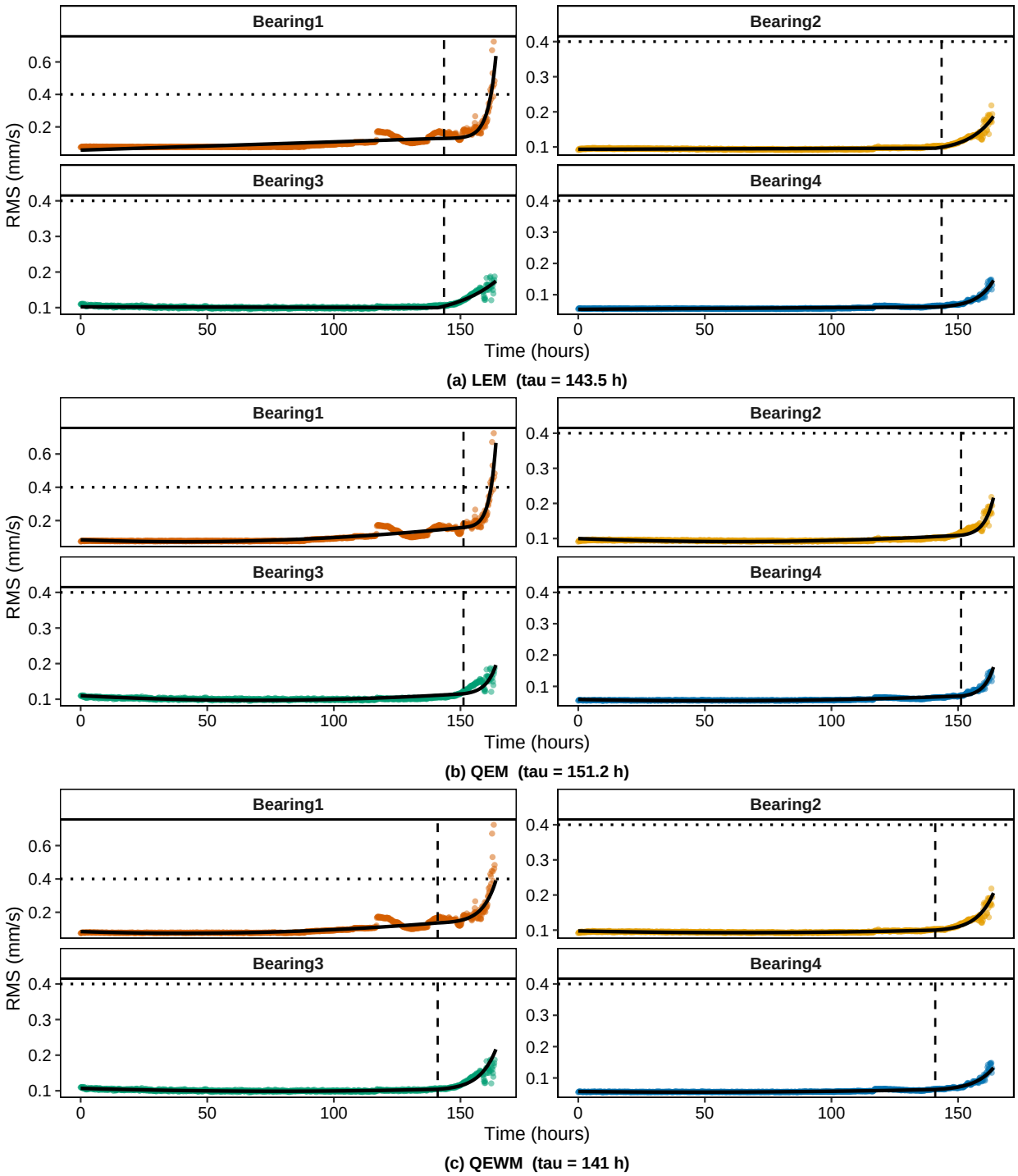

Figure 2. Model fitting results for the three candidate models.

The core optimization is executed via the `nlme()` function, incorporating the `varPower(form = ~ fitted(.))` variance function structure. This specification directly parameterizes the heteroscedastic power parameter δ defined in (7), enabling automatic, dynamic weight calculation based on the model-predicted values $\hat{Y}_i(t)$. Consequently, this algorithmic setup effectively realizes the variance-weighted statistical framework proposed in this study.

5. RESULTS AND MODEL COMPARISON

5.1. Degradation Path Fitting

The proposed modeling framework is evaluated by comparing three candidate models: the linear exponential model (LEM), the quadratic exponential model (QEM), and the quadratic exponential weighted model (QEWM). While all models share the same two-stage structure defined in (3), they differ fundamentally in the functional form of the early-stage mean path ($D_{1,i}(t)$) and the **variance structure of the random error term** $\varepsilon_i(t)$ governed by the parameter δ in (7):

1. **LEM (Linear Exponential Model):**
   - **Early-stage mean path:** $D_{1,i}(t) = \alpha_{0,i} + \alpha_{1,i}t$, representing a linear baseline trend.
   - **Error variance structure:** $\delta = 0$, implying **homoscedastic errors** where $\text{Var}(\varepsilon_i(t)) = \sigma^2$. The measurement uncertainty is assumed to be constant across all degradation levels.
2. **QEM (Quadratic Exponential Model):**
   - **Early-stage mean path:** $D_{1,i}(t) = \alpha_{0,i} + \alpha_{1,i}t + \alpha_{2,i}t^2$, which accounts for mild curvature in the early phase.
   - **Error variance structure:** $\delta = 0$, assuming **homoscedasticity** regardless of the increasing vibration severity.
3. **QEWM (Quadratic Exponential Weighted Model):**
   - **Early-stage mean path:** Utilizes the same quadratic structure as the QEM.
   - **Error variance structure:** δ is treated as an **estimated parameter** ($\delta = 3.03$ in Table 2). This defines a **heteroscedastic error structure**, $\text{Var}(\varepsilon_i(t)) = \sigma^2|\hat{Y}_i(t)|^{2\delta}$, where the variability of the random error term scales with the predicted RMS magnitude.

The QEWM corresponds to the complete two-stage nonlinear mixed-effects model presented in Eqs. (3)–(6). By explicitly modeling the variance structure of the error term, the QEWM effectively prevents the estimation from being dominated by high-variance observations in the late degradation stage, ensuring a more robust statistical inference.

Figure 2 illustrates the fitted degradation trajectories overlaid with the observed RMS paths. The LEM captures the general increasing trend but fails to adequately represent the curvature observed in the early degradation stage. Introducing a quadratic term in the QEM improves the fit during the early stage; however, noticeable discrepancies remain in the late-stage region, particularly near failure.

The QEWM provides the most consistent fit across both degradation stages. By incorporating the weighted variance structure, the model avoids excessive influence from highly variable late-stage observations, resulting in a smoother and more stable representation of the underlying degradation process.

5.2. Residual Diagnostics

Residual diagnostics further highlight the differences among the three models, as shown in Figure 3. For both LEM and QEM, residual plots exhibit a clear heteroscedastic pattern, with residual dispersion increasing markedly as the predicted RMS level rises. This behavior is particularly pronounced during the late degradation stage, indicating a violation of the homoscedasticity assumption.

In contrast, the QEWM substantially mitigates this issue. After accounting for the variance structure, the standardized residuals display no systematic dependence on the predicted RMS level, and their dispersion remains approximately constant across time. These results confirm that the weighted variance formulation effectively captures the heteroscedastic nature of the degradation data.

5.3. Model Selection

Quantitative model comparison is conducted using the Akaike Information Criterion (AIC). Table 1 summarizes the AIC values for the three candidate models. Among them, the QEWM consistently yields the lowest AIC, indicating superior goodness-of-fit after accounting for model complexity.

Importantly, the improved AIC performance of the QEWM is not solely driven by increased flexibility in the mean structure but arises primarily from its ability to appropriately model the variance behavior. This finding underscores the importance of explicitly addressing heteroscedasticity in vibration-based degradation modeling.

Table 1. Comparison of the three candidate degradation models based on AIC.

Model	AIC	LogLik	Parameters
LEM	-23609.80	11812.90	8
QEM	-24700.48	12360.24	10
QEWM	**-31719.67**	15870.84	11

As shown in Table 2, the fixed effects estimates under the QEWM reveal significant results for the parameters. The reported p-values correspond to the asymptotic Wald tests under the following hypotheses:

$$H_0 : \eta = 0$$
$$H_1 : \eta \neq 0$$

where $\eta \in \{\beta_0, \beta_1, \beta_2, \beta_3, \theta\}$. All primary parameters exhibit high statistical significance ($p < 0.05$), validating the necessity of including both the quadratic baseline curvature and the exponential acceleration component. Furthermore, Table 3 presents the estimated standard deviations of the ran-

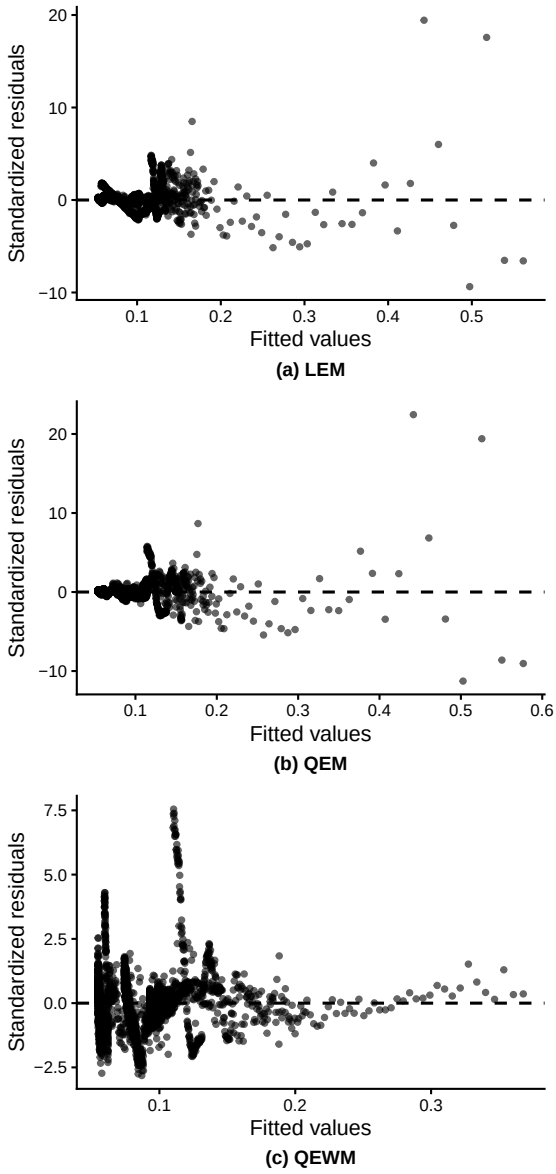

Figure 3. Residual diagnostics for the three candidate models.

dom effects and the residual term, reflecting the variability in bearing degradation dynamics and the remaining unexplained variation.

6. LIFETIME PREDICTION AND UNCERTAINTY QUANTIFICATION

6.1. Monte Carlo Degradation Simulation

To estimate bearing lifetime distributions, Monte Carlo simulation is conducted based on the fitted QEWM. For each simulation run, bearing-specific random effects are sampled from the estimated random-effects distribution, and residual variability is generated according to the weighted variance structure. The resulting degradation paths represent plausible realizations of bearing behavior under the modeled uncertainty.

Table 2. Estimates of fixed effects under the QEWM

Effect	Value	Standard error	p-value
β_0	8.64×10^{-2}	9.46×10^{-3}	< 0.0001
β_1	-2.35×10^{-4}	8.09×10^{-5}	0.0037
β_2	2.40×10^{-6}	1.10×10^{-6}	0.0287
β_3	1.57×10^{-1}	1.17×10^{-2}	< 0.0001
θ	3.37×10^{-3}	3.41×10^{-4}	< 0.0001
δ	3.03	–	–

Table 3. Estimated standard deviations of random effects under the QEWM

Effect	Estimated standard deviation
$b_{0,i}$	1.89×10^{-2}
$b_{1,i}$	1.61×10^{-4}
$b_{2,i}$	2.19×10^{-6}
$b_{3,i}$	2.03×10^{-2}
Residual	6.71

The failure time for each simulated path is defined as the first passage time at which the RMS trajectory exceeds the predefined failure threshold of 0.4 mm/s. Repeating this procedure yields an empirical distribution of bearing lifetimes.

Figure 4 presents the degradation paths cloud for the four bearings, along with the estimated lifetime probability density function (PDF) under the QEWM model. Each line represents a degradation trajectory of one bearing, showing how its RMS evolves over time. The shaded area illustrates the distribution of simulated degradation paths, accounting for the bearing-specific random effects and residual variability.

The PDF curve captures the estimated lifetime distribution, providing insights into the likelihood of failure at each time point. The failure threshold of 0.4 mm/s is indicated, marking the point at which failure occurs. This figure provides a visual representation of the uncertainty in the lifetime estimates and the variability of degradation paths under the model.

6.2. Reliability Metrics

From the simulated lifetime distribution, standard reliability metrics are derived. In particular, the reliability function and cumulative distribution function (CDF) are constructed, and the B10 life is estimated as the time corresponding to a 10% failure probability.

The estimated B10 life provides a conservative reliability measure commonly adopted in industrial maintenance planning. The results indicate that the proposed QEWM produces stable and interpretable lifetime estimates consistent with observed degradation behavior.

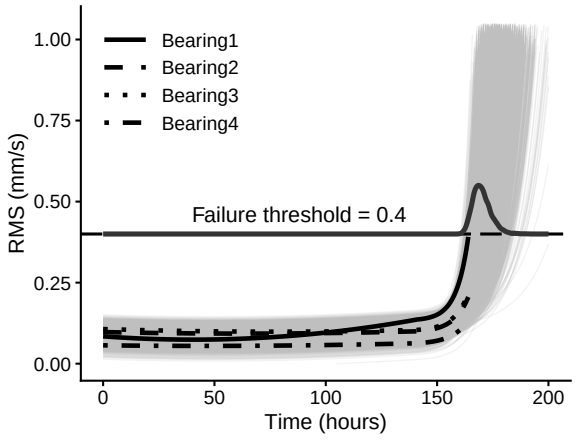

Figure 4. Degradation paths cloud and estimated lifetime PDF under the QEWM.

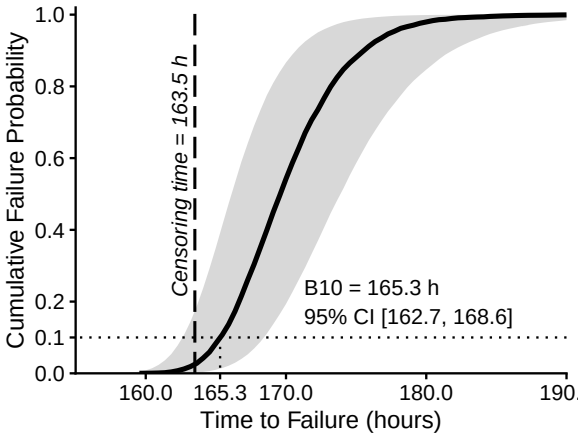

Figure 5. Estimated CDF of the lifetime under the QEWM.

6.3. Bootstrap Confidence Intervals

To quantify uncertainty arising from parameter estimation, bootstrap techniques are employed (Efron & Tibshirani, 1994; Meeker et al., 2021). Parametric bootstrap resampling is performed by repeatedly generating synthetic datasets from the fitted model and re-estimating parameters for each replicate. For each bootstrap sample, Monte Carlo simulation is repeated to obtain a corresponding lifetime distribution.

Confidence intervals for the B10 life are then constructed from the empirical distribution of bootstrap estimates. This procedure captures uncertainty originating from both model parameters and stochastic degradation dynamics, providing a comprehensive assessment of lifetime uncertainty.

Figure 5 presents the estimated CDF of the lifetime under the QEWM. The solid line represents the model's estimated CDF, while the shaded region indicates the 95% bootstrap confidence interval for the lifetime distribution.

The B10 life is estimated to be 165.3 hours, with a 95% confidence interval of [162.7, 168.6] hours. This estimate provides a conservative prediction of the lifetime, where the B10 life refers to the time by which 10% of the bearings are expected to fail. The 95% CI for the B10 life indicates the uncertainty around this estimate, offering a range in which the true B10 life is likely to fall, considering variability in the degradation process.

Furthermore, the shaded area around the CDF curve represents the 95% CI for the CDF, capturing the uncertainty in the cumulative failure probability across all time points. This highlights the spread of the failure times, providing further insight into the reliability of the lifetime predictions derived from the model.

7. DISCUSSION

The results demonstrate that explicitly modeling phase transition and heteroscedasticity is essential for reliable bearing degradation analysis. While simpler two-stage models can capture the overall degradation trend, they tend to be dominated by highly variable late-stage observations, leading to unstable parameter estimates and inflated uncertainty. By incorporating a weighted variance structure, the proposed QEWM effectively mitigates this issue and yields more stable degradation trajectories and lifetime estimates.

An important advantage of the proposed framework lies in its interpretability. Each model component corresponds to a physically meaningful aspect of bearing degradation: the early-stage polynomial term represents gradual wear under normal operation, the late-stage exponential term captures rapid defect propagation prior to failure, and the random effects quantify bearing-to-bearing variability. This interpretability distinguishes the proposed approach from purely data-driven methods and aligns well with practical PHM requirements.

The inclusion of random effects plays a critical role in lifetime uncertainty quantification. Under a nonlinear mixed-effects framework, the variability is properly decomposed into population-level, unit-to-unit (random effects), and within-unit (residual error) components. If these random effects are neglected (i.e., treating the pooled data with a simple fixed-effects model), the residual variance would artificially inflate to absorb the unexplained unit-to-unit heterogeneity. Consequently, this variance inflation would lead to severely overestimated and unrealistic confidence intervals for the overall reliability metrics, while failing to accurately capture individual bearing failure risks.

Several limitations of the present study should be acknowledged. First, the analysis is conducted using a single benchmark dataset, and the number of bearings is limited. While this dataset provides a representative degradation scenario with

both failed and censored units, future studies should evaluate the proposed framework on additional bearing datasets and operating conditions. Second, the change point τ is treated as a tuning parameter selected by information criteria rather than a fully inferred random variable. While this grid-search approach is computationally pragmatic and ensures numerical stability, it does not propagate the uncertainty of the change-point estimation into the final lifetime predictions. To enhance methodological rigor, future research could modify the formulation by directly incorporating the change point τ as an unknown parameter inside the likelihood function for joint estimation. This modification would allow the simultaneous extraction of the asymptotic standard error for τ, thereby seamlessly integrating its estimation uncertainty into the downstream prognostic assessments.

Despite these limitations, the proposed framework offers a practical and extensible solution for degradation-based bearing reliability analysis. The modeling strategy is not specific to the IMS dataset and can be readily applied to other PHM applications involving phase-transition behavior and heteroscedastic degradation signals.

8. CONCLUSION

This study presents a two-stage nonlinear mixed-effects degradation modeling framework with a weighted variance structure for bearing reliability analysis. By explicitly accounting for phase-transition behavior, bearing-to-bearing variability, and heteroscedastic degradation signals, the proposed approach provides a robust and interpretable solution for vibration-based prognostics.

Application to the IMS bearing dataset demonstrates that incorporating variance weighting substantially improves model adequacy, residual behavior, and lifetime uncertainty quantification. The resulting B10 life estimates and confidence intervals offer meaningful and conservative reliability metrics suitable for practical maintenance planning.

Overall, the proposed framework bridges statistical rigor and practical applicability, making it a valuable tool for PHM applications where degradation dynamics exhibit both structural transitions and non-constant variability.

REFERENCES

Akaike, H. (1974). A new look at the statistical model identification. *IEEE Transactions on Automatic Control*, *19*(6), 716–723. doi: 10.1109/TAC.1974.1100705

Davidian, M., & Giltinan, D. M. (1995). *Nonlinear models for repeated measurement data*. New York: Chapman & Hall.

Efron, B., & Tibshirani, R. J. (1994). *An introduction to the bootstrap*. New York: CRC Press.

Gebraeel, N., Lawley, M., Li, R., & Ryan, J. K. (2005). Residual-life distributions from component degradation signals: A Bayesian approach. *IIE Transactions*, *37*(6), 543–557. doi: 10.1080/07408170590929018

IMS Center. (2004). *IMS bearing dataset.* `https://www.imscenter.net`. (NSF I/UCR Center for Intelligent Maintenance Systems)

International Organization for Standardization. (2022). *Mechanical vibration—measurement and evaluation of machine vibration—part 3: Industrial machines with nominal power above 15 kW and nominal speeds between 120 r/min and 30 000 r/min when measured in situ (ISO 20816-3:2022).* `https://www.iso.org/standard/78189.html`. (Geneva, Switzerland)

Lee, J., Wu, F., Zhao, W., Ghaffari, M., Liao, L., & Siegel, D. (2014). Prognostics and health management design for rotary machinery systems—reviews, methodology and applications. *Mechanical Systems and Signal Processing*, *42*(1-2), 314–334. doi: 10.1016/j.ymssp.2013.06.004

Lin, J., Liao, G., Chen, M., & Yin, H. (2021). Two-phase degradation modeling and remaining useful life prediction using nonlinear Wiener process. *Computers & Industrial Engineering*, *160*, 107533. doi: 10.1016/j.cie.2021.107533

Lindstrom, M. J., & Bates, D. M. (1990). Nonlinear mixed effects models for repeated measures data. *Biometrics*, *46*(3), 673–687.

Meeker, W. Q., Escobar, L. A., & Pascual, F. G. (2021). *Statistical methods for reliability data* (2nd ed.). Wiley.

Meng, Z., Li, J., Yin, N., & Pan, Z. (2020). Remaining useful life prediction of rolling bearing using fractal theory. *Measurement*, *161*, 107572. doi: 10.1016/j.measurement.2020.107572

Rubinstein, R. Y., & Kroese, D. P. (2017). *Simulation and the Monte Carlo method* (3rd ed.). Wiley.

Wang, L., & Gao, R. X. (2006). *Condition monitoring and control for intelligent manufacturing*. London: Springer.